Supplementary materials

Experimental sections

1. Products analysis

Qualitative analysis of the products was conducted using a gas chromatography/mass spectrometry (GC-MS) system equipped with a HP-INNOWAX column (30 m in length, 0.25 mm in diameter, and 0.25 mm in film thickness). Initially, the oven temperature was raised to 60 °C and held for 2 min, followed by a programmed increase to 160 °C at a rate of 10 °C/min and maintained for an additional 10 minutes. Helium served as the carrier gas, with a split ratio of 5:1. For further measurement, the products were analyzed by a gas chromatography instrument (SHIMADZU GC-2030) equipped with a flame ionization detector (FID) and a thermal conductivity detector (TCD). The oven temperature program for the GC-MS analysis was adhered to. The conversion of FF, yield of FA, and selectivity towards FA were calculated using the following formulas:

$$FF\ conversion = \frac{Initial\ mole\ of\ FF - Final\ mole\ of\ FF}{Initial\ mole\ of\ FF} \qquad (1)$$

$$FA\ yield = \frac{Mole\ of\ product}{Theoreticle\ mole\ of\ product} \qquad (2)$$

$$FA\ selectivity = \frac{FA\ yield}{FF\ conversion} \qquad (3)$$

2. Characterization of catalyst

The Zr-chitin samples underwent N_2 adsorption-desorption isotherms analysis using a Micromeritics ASAP 2020 instrument. Prior to analysis, the catalyst was pretreated at 120 °C for 6 hours to eliminate adsorbed water. The BET method was employed to measure the surface area of the catalyst, while the pore volume and size were determined using the BJH method. X-ray photoelectron spectroscopy (XPS) was conducted on a Leybold LH 10 spectrometer equipped with a single-channel detector under vacuum conditions. X-ray diffraction patterns (XRD) were recorded using a Rigaku diffractometer with Cu Kα radiation ($\lambda = 0.154$ nm) over a scanning angle range of 10° to 80°. Scanning electron microscopy (SEM) images were captured using a

ZEISS GeminiSEM 300 instrument at 15 kV. Transmission electron microscope (TEM) and energy dispersive spectrometry (EDS) analyses were performed on a Talos F200X G_2 instrument, operating at 15 kV. Fourier transform infrared spectroscopy (FT-IR) was conducted on a Nicolet iS50 FT-IR spectrometer to identify functional groups. Pyridine adsorption FT-IR measurements were carried out on a Nicolet iS50 FT-IR spectrometer equipped with an MCT detector, with 128 scans and a resolution of 2 cm^{-1}, over a wavelength range of 4000 to 400 cm^{-1}, to determine acid sites. The acid-base properties of the catalyst were evaluated via temperature-programmed adsorption-desorption of CO_2 or NH_3 (CO_2-TPD or NH_3-TPD) using a Microtrac BELCat analyzer. Prior to analysis, the sample was heated to 150 °C and maintained for 2 hours to remove adsorbed water, followed by cooling to room temperature under a flowing He (30 mL/min). After adsorption of excess CO_2 or NH_3 at 50 °C, the temperature was increased to 300 °C at a rate of 10 °C/min under a flowing He (30 mL/min). The thermal stability of the catalyst was assessed using a Swiss Mettler Toledo thermal analyzer (TG), with the temperature increased from 30 °C to 800 °C under a flowing Ar at a rate of 15 °C/min. The Zr content in the catalysts was measured using ICP-OES equipment (Agilent ICP-OES 720).

3. Activity tests

The activity tests were performed in a 10 mL pressure tube reactor in oil-heating condition. Typically, 0.5 mmol FF, 5 mL IPA and 50 mg catalyst were added into the pressure tube reactor. Then the pressure tube reactor was placed into pre-set temperature oil bath. After the reaction, the reactor was cooled to room temperature and the mixtures were centrifuged and the used catalysts were collected for the recycling experiments.

4. Isotopic labelled experiments

For isotopic kinetic investigation of FF to FA, we employed deuterium-labeled 2-PrOH-d_8 as a hydrogen source to elucidate reaction mechanisms and rate-determining steps. After the reaction, the reaction mixtures were analyzed by GC–MS.

5. Catalyst recycling experiment

The reusability test of Zr-Ch (3:1) catalyst was performed as follows: After the reaction proceeded at 100 °C for 2 h, the solid Zr-Ch (3:1) was separated by centrifugation, and washed several times with 2-PrOH. After dried under vacuum at 60 °C for 12 h, the Zr-Ch (3:1) was employed for the next cycle directly under the identical reaction conditions.

6. Isotopic labelled experiments

For isotopic kinetic investigation of FF to FA, we employed deuterium-labeled 2-propanol 2-PrOH-d_8 as a hydrogen source to elucidate reaction mechanisms and rate-determining steps. After the reaction, the products were measured by GC-MS (Thermo TRACE QP2010 SE).

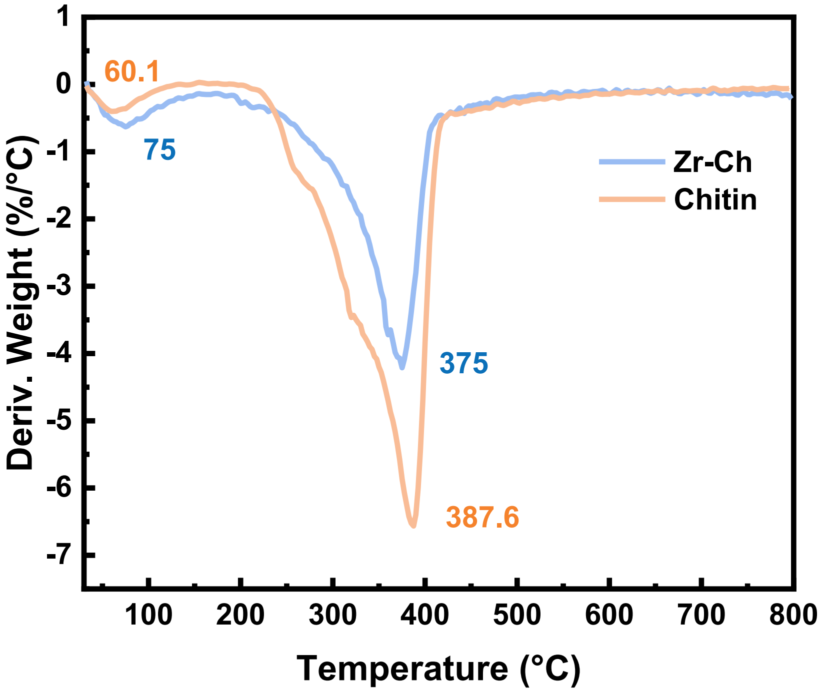

Figure S1 DTG curve of various catalysts

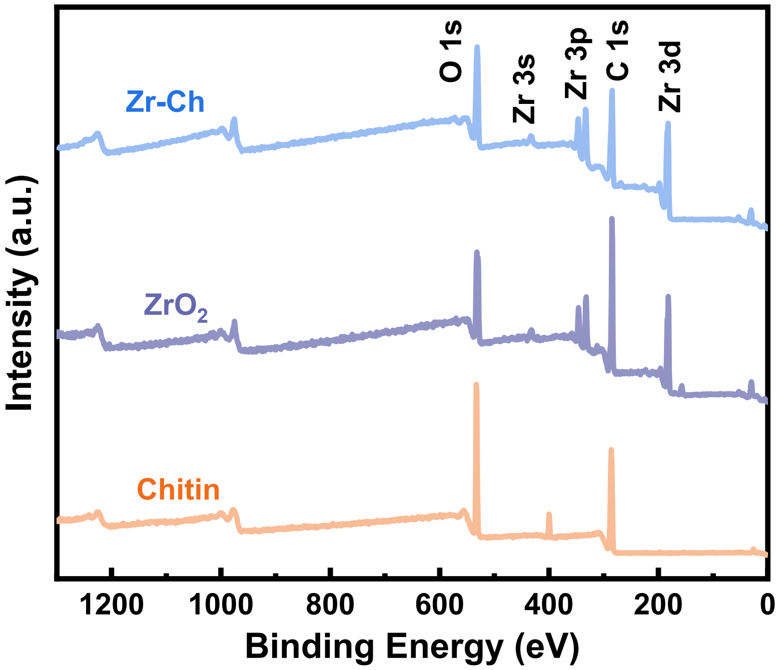

Figure S2 The XPS spectra of Zr-Ch (3:1), ZrO_2 and chitin

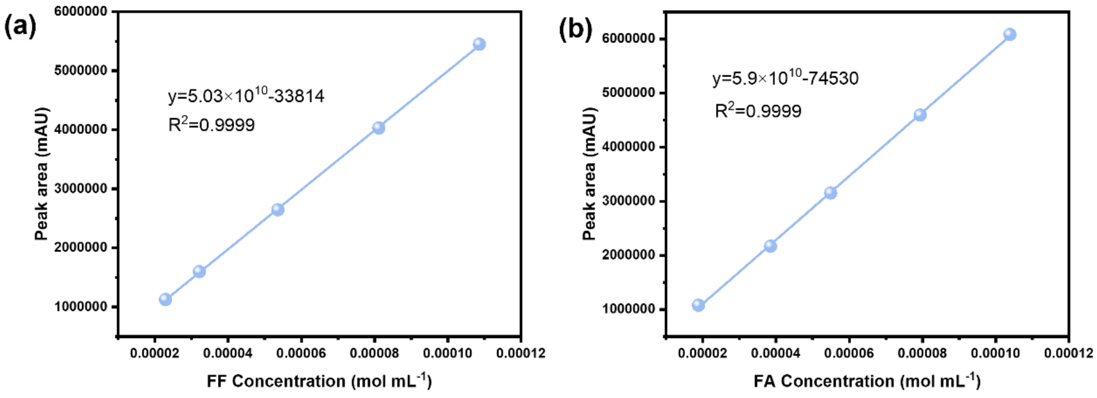

Figure S3 Standard curve of FF (a) and FA(b)

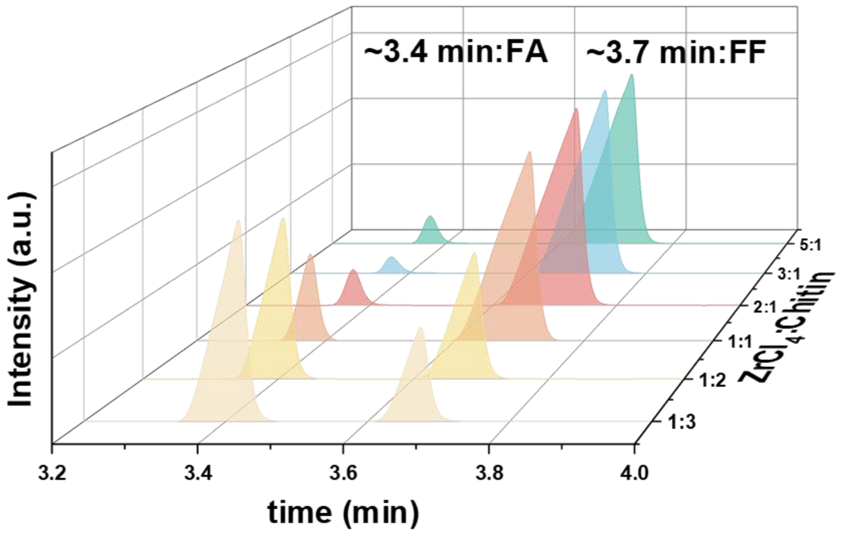

Figure S4 GC chromatogram of effects of proportion of Zr in catalyst on MPV reduction of

FF to FA

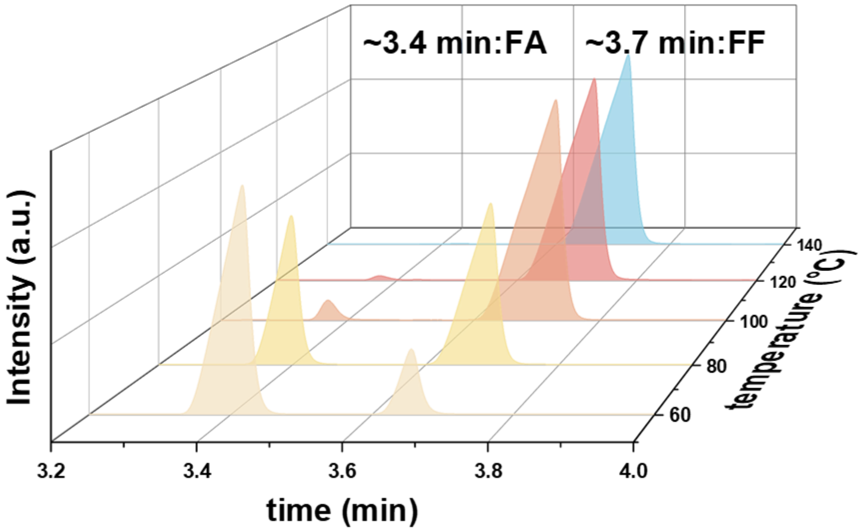

Figure S5 GC chromatogram of effects of reaction time on MPV reduction of FF to FA

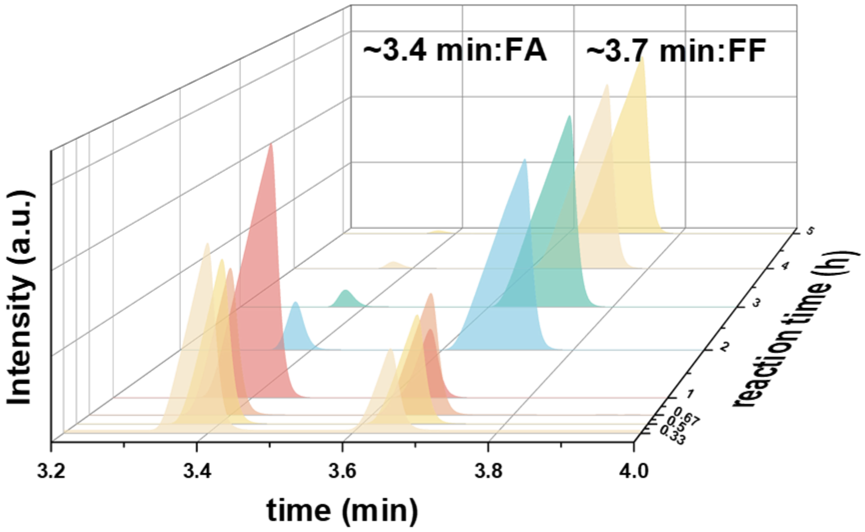

Figure S6 GC chromatogram of effects of temperature on MPV reduction of FF to FA

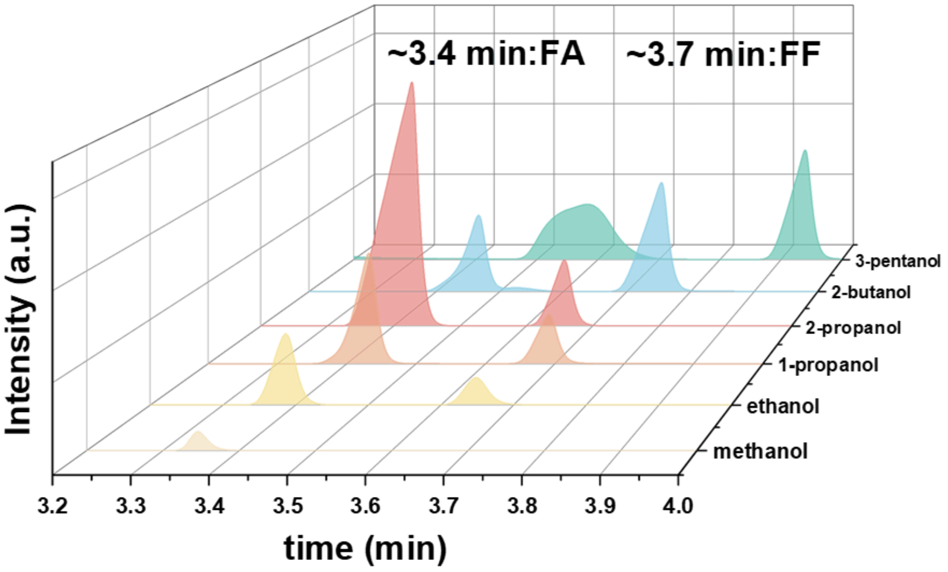

Figure S7 GC chromatogram of hydrogen donor on MPV reduction of FF to FA

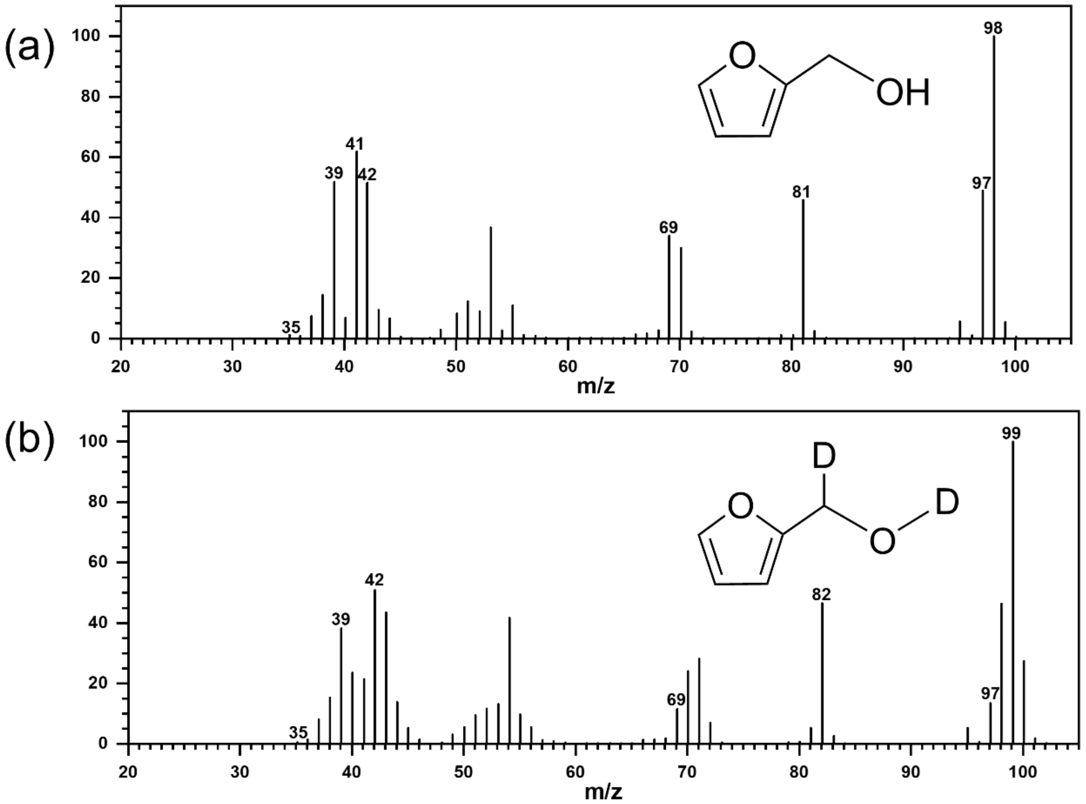

Figure S8 MS spectra of (a) FA production in IPA, (b) FF product in 2-PrOH-d_8

Table S1 BET surface area, pore volume and pore radius of Zr-Ch (3:1) and ZrO_2

Catalysts	SBET (m^2/g)	Pore volume (cm^3/g)	Average pore diameter (nm)
Zr-Ch (3:1)	101.2	0.20	10.49
ZrO_2	8.3	0.07	0.07

Table S2 Acid-base properties of various catalysts by NH_3/CO_2-TPD

Catalyst	Acid sites		Base sites		Acid/Base ratio
	Content (mmol/g)	Desorption time	Content (mmol/g)	Desorption time	
Zr-Ch (3:1)	0.628	90	0.109	90	5.76
ZrO_2	0.01	-	0.01	-	1

Table S3 Acid properties of catalysts by pyridine-adsorbed FT-IR spectra

Catalyst	150 °C		225 °C	
	B(mmol/g)	L(mmol/g)	B(mol/g)	L(mol/g)
Zr-Ch (3:1)	0.01565	0.13133	0.01136	0.03870
Chitin	0.03304	0.09749	0.02446	0.02700

Table S4 MPV of FF to FA with various catalysts

	Catalyst	Temp (°C)	Time (h)	FF Conv. (%)	FA Yield (%)	FA Sele. (%)
1	chitin	100	3	0	0	0
2	ZrO_2	100	3	1.0	4.2	0
3	Zr-Ch (1:1)	100	3	78.8	74.2	94.2
4	Zr-Ch (1:2)	100	3	43.3	40.9	94.4
5	Zr-Ch (2:1)	100	3	90.9	90.4	99.4
6	Zr-Ch (1:3)	100	3	26.4	24.6	93.2
7	Zr-Ch (3:1)	100	3	95.5	94.9	98.9
8	Zr-Ch (5:1)	100	3	91.4	90.4	98.9
9[a]	Zr-Ch (3:1)	100	3	11.7	3.6	30.6
10[b]	Zr-Ch (3:1)	100	3	62.5	50.8	81.3
11[c]	Zr-Ch (3:1)	100	3	96.1	94.4	98.2

a: Base sites of Zr-Ch (3:1) were poisoned by adding 50 mg benzoic acid;

b: Acid sites of Zr-Ch (3:1) were poisoned by adding 50 mg pyridine;

c: Brønsted acid sites of Zr-Ch (3:1) were poisoned by adding 50 mg 2,6-lutidine.

Table S5 ICP and Elemental analysis of fresh and used catalysts

Catalyst	Zr
Zr-Ch (3:1)-fresh	41.55
Zr-Ch (3:1)-used	43.27

Table S6 Effect of solvent on MPV of FF catalyzed by Zr-Ch (3:1)

Entry	Catalyst	Solvent	Time (h)	FF Conv. (%)	FA Yield (%)	FA Sele. (%)
1	Zr-Ch (3:1)	methanol	3	94.0	0	0
2	Zr-Ch (3:1)	ethanol	3	80.5	50.5	73.7
3	Zr-Ch (3:1)	1-propanol	3	57.87	78.6	82.4
4	Zr-Ch (3:1)	2-propanol	3	95.5	94.9	98.9
5	Zr-Ch (3:1)	2-butanol	3	70.3	36.3	51.7
6	Zr-Ch (3:1)	tert-butanol	3	8.2	3.4	42.0
7	Zr-Ch (3:1)	3-pentanol	3	48.0	30.5	63.5

Reaction condition: 0.5 mmol FF in 5 ml IPA, 50 ml catalyst, 100 °C, 3 h.

Table S7 Activation energy of FF to FA with various catalysts

Entry	Catalyst	Activation energy(kJ/mol)	Ref.
1	Zr-Ch	22.17	This work
2	$Al_7Zr_3@Fe_3O_4$	45.3	[1]
3	$NiFe_2O_4$	48.2	[2]
4	Zr-LS	52.25	[3]
5	ZrPN	70.5	[4]
6	Mn-NCA-700	83	[5]

[1] HE Jian, YANG Song, RIISAGER A. Magnetic nickel ferrite nanoparticles as highly durable catalysts for catalytic transfer hydrogenation of bio-based aldehydes [J]. Catalysis Science & Technology, 2018, 8(3): 790–797.

[2] [2] HE Jian, YANG Song, RIISAGER A. Magnetic nickel ferrite nanoparticles as highly durable catalysts for catalytic transfer hydrogenation of bio-based aldehydes [J]. Catalysis Science & Technology, 2018, 8(3): 790–797.

[3] ZHOU Sheng-hui, DAI Fang-lin, XIANG Zhou-yang, et al. Zirconium – lignosulfonate polyphenolic polymer for highly efficient hydrogen transfer of biomass-derived oxygenates under mild conditions [J]. Applied Catalysis B: Environmental, 2019, 248: 31–43. DOI:10.1016/j.apcatb.2019.02.011.

[4] SONG Jin-liang, ZHOU Bao-wen, ZHOU Hua-cong, et al. Porous zirconium–phytic acid hybrid: A highly efficient catalyst for meerwein – ponndorf – verley reductions [J]. Angewandte Chemie International Edition, 2015, 54(32): 9399–9403. DOI:10.1002/anie.201504001.

[5] PANAGIOTOPOULOU P, MARTIN N, VLACHOS D G. Inside cover: Liquid-phase catalytic transfer hydrogenation of furfural over homogeneous lewis acid–Ru/C catalysts (ChemSusChem 12/2015) [J]. ChemSusChem, 2015, 8(12): 1990. DOI:10.1002/cssc.201500748.